

A Variant of the Nonlinear Multiscale Dynamic Diffusion Method

Andrea M. P. Valli[1], Isaac P. Santos[2], Sandra M. C. Malta[3], Lucia Catabriga[1(✉)], and Regina C. Almeida[3]

[1] DI, Universidade Federal do Espírito Santo, Vitória, ES, Brazil
{avalli,luciac}@inf.ufes.br
[2] DMA, Universidade Federal do Espírito Santo, São Mateus, São Mateus, ES, Brazil
isaac.santos@ufes.br
[3] Laboratório Nacional de Computação Científica, Petrópolis, RJ, Brazil
{smcm,rcca}@lncc.br

Abstract. This paper presents a two-scale finite element formulation for a variant of the nonlinear Dynamic Diffusion (DD) method, applied to advection-diffusion-reaction problems. The approach, named here new-DD method, introduces locally and dynamically an extra stability through a nonlinear operator acting in all scales of the discretization, and it is designed to be bounded. We use bubble functions to approximate the subgrid scale space, which are locally condensed on the resolved scales. The proposed methodology is solved by an iterative procedure that uses the bubble-enriched Galerkin solution as the correspondent initial approximation, which is automatically recovered wherever stabilization is not required. Since the artificial diffusion introduced by the new-DD method relies on a problem-depend parameter, we investigate alternative choices for this parameter to keep the accuracy of the method. We numerically evaluate stability and accuracy properties of the method for problems with regular solutions and with layers, ranging from advection-dominated to reaction-dominated transport problems.

Keywords: New-dynamic diffusion method · Bubble functions · Advection-diffusion-reaction equations

1 Introduction

Stable finite element approximations to advection-diffusion-reaction problems have been the subject of intense research for the past forty years. Typical Galerkin formulations for this class of problems lack stability when advection or reaction effects are much stronger than the diffusion phenomena. Several works proposed the introduction of stabilization along the streamlines, in a linear and consistent manner [2,11,14]. To deal with instabilities along other directions, a variety of nonlinear stabilization methodologies have been developed [4,12,13,16]. Both linear

Supported by organizations CNPq, FAPERJ and FAPES.

© Springer Nature Switzerland AG 2021
O. Gervasi et al. (Eds.): ICCSA 2021, LNCS 12949, pp. 48–61, 2021.
https://doi.org/10.1007/978-3-030-86653-2_4

and nonlinear stabilization terms depend on user-defined parameters that ultimately yield the accuracy and stability properties of the method. More recently, the broader framework introduced by variational multiscale finite element formulations [8,9] have reformulated stabilized methods by decomposing state variables into resolved and unresolved (subgrid) scales. In the multiscale framework, stabilized methods can be seen as techniques to capture the unresolved scale variability into the resolved scale solution. Such an approach has opened new directions of research. The method proposed in [7], for example, used scale separation to introduce artificial dissipation only onto the small scales, still requiring definition of tunable parameter. This drawback was overcome in [17] by using a subgrid diffusivity stabilization that locally depends on the resolved scale solution. Using the same basis for the construction of stabilization, this method was extended in [1] by adding isotropic dissipation on all scales, in the context of non conforming two-scale methods. The so called Dynamic Diffusion (DD) method was then extended to the continuous setting in [19,20] by using bubble functions to build the subgrid space. In this way, the subgrid degrees of freedom can be condensed onto the resolved scale degrees of freedom, reducing the computational cost typical of two-scale methods. The resulting technique shows robust stability properties for advection-diffusion-reaction problems in the presence of layers [20].

In the DD model, a nonlinear dissipation mechanism is introduced in both the resolved and unresolved scales. The artificial diffusion is dynamically evaluated depending on the resolved scale solution. Specifically, it depends on the residual and the gradient of the resolved scale solution, as well as on a characteristic local length scale. In this way, without invoking any linear stabilization, the DD method does not require any additional user-defined parameter and ultimately avoids kinetic energy accumulation at the resolved scale, precluding local and non-local oscillations in the presence of layers. Unfortunately, the numerical analysis of the DD method could not be established since the artificial diffusion operator is not upper bounded, a key issue to prove the existence of discrete solution, stability, and *a priori* error estimate. To overcome this drawback, a new-DD method was developed and analyzed in [18], and optimal convergence rates in the $L^2(\Omega)$, $H^1(\Omega)$, and energy norms were numerically shown for problems with smooth solutions.

Here, we investigate the behavior of the new-DD method for problems with internal and external layers, ranging from advection dominated to reaction dominated transport problems. Of note, the artificial diffusion introduced by the new-DD method relies on a problem dependent parameter that plays a key role on its upper boundedness. Although it can be defined locally and depending on the problem, we perform numerical experiments to investigate alternative, and eventually simpler, choices for this parameter that does not compromise the accuracy of the method. Thus, focusing on those numerical aspects, this work is organized as follows. In Sect. 2 we present the new-DD method for solving the advection-diffusion-reaction transport problems. Section 3 contains the numerical studies and the evaluation of the method. The conclusions are summarized in Sect. 4.

2 The New Dynamic Diffusion Method

The problem of interest is modeled by the following steady-state advection-diffusion-reaction equation

$$-\epsilon\,\Delta u + \boldsymbol{\beta}\cdot\boldsymbol{\nabla} u + \sigma u = f, \qquad \text{in } \Omega, \tag{1}$$

where the domain $\Omega \subset \mathbb{R}^2$ has a sufficiently regular boundary Γ. It represents the transport dynamics of a scalar field u (e.g., temperature, chemical concentration, etc.), subject to the diffusion coefficient $\epsilon > 0$ and to the incompressible velocity field $\boldsymbol{\beta}$. Local dynamics are modeled by the reaction term σu, in which $\sigma \geq 0$ is the reaction coefficient; and f is the source term. To complete the problem setting, we assume for simplicity the following homogeneous Dirichlet boundary conditions

$$u = 0, \qquad \text{on } \Gamma. \tag{2}$$

Also for simplicity, and without loss of generality, we assume that both ϵ and σ are constant parameters. From now on we use $H^1(X)$ to denote the Hilbert space in X, for each $X \subseteq \Omega$, and $H^0(X) = L^2(X)$. We also denote $\|\cdot\|_{m,X}$ as the standard norm in $H^1(X)$ $(m = 1)$ and in $L^2(X)$ $(m = 0)$, and $(\cdot,\cdot)$ as the inner product in $L^2(X)$.

A general variational formulation of problem (1)–(2) is: find $u \in H_0^1(\Omega) = \{u \in H^1(\Omega), u = 0 \text{ on } \Gamma\}$ such that

$$B(u, v) = (f, v), \quad \forall v \in H_0^1(\Omega), \tag{3}$$

with

$$B(u, v) = \epsilon(\boldsymbol{\nabla} u, \boldsymbol{\nabla} v) + (\boldsymbol{\beta}\cdot\boldsymbol{\nabla} u, v) + \sigma(u, v). \tag{4}$$

To build the corresponding discrete multiscale formulation we first define a regular triangulation $\mathcal{T}_h = \{T\}$ of the domain Ω into regular elements, denoted by T, and we set $h = \max\{h_T : T \in \mathcal{T}_h\}$ with $h_T := diam(T)$. The Galerkin formulation associated to (3) consists of finding $u_h \in V_h^0 \subset H_0^1(\Omega)$ such that

$$B(u_h, v_h) = (f, v_h), \quad \forall v_h \in V_h^0, \tag{5}$$

where $V_h^0 = \{w \in H^1(\Omega) \mid w|_T \in \mathbb{P}_1(T),\ \forall T \in \mathcal{T}_h,\ w|_\Gamma = 0\}$, with $\mathbb{P}_1(T)$ the set of first order polynomials in elements $T \in \mathcal{T}_h$. In the multiscale framework, we consider that V_h^0 is the resolved (grid) scale space, and we define the two-scale approximation space $V_{hb}^0 = V_h^0 \oplus V_b$, which is a direct sum of V_h^0 and an unresolved subgrid (fine) scale space V_b. As in [7], we define $V_b = \{v_b \in H_0^1(\Omega);\ v_b|_T = span\{\psi_T\}, \forall T \in \mathcal{T}_h\}$, where $\psi_T \in H_0^1(T)$ are bubble functions. Specifically, we define $\psi_T(\boldsymbol{x}) = 27N_1(\boldsymbol{x})N_2(\boldsymbol{x})N_3(\boldsymbol{x})$, $\forall \boldsymbol{x} \in T$, where N_i is the basis function associated of the i^{th} node of T. Using these definitions, the new-DD method consists of finding $u_{hb} = u_h + u_b \in V_{hb}^0$, with $u_h \in V_h^0$, $u_b \in V_b$, such that

$$B(u_{hb}, v_{hb}) + \sum_{T\in\mathcal{T}_h} D_T(u_{hb}; u_{hb}, v_{hb}) = (f, v_{hb}), \quad \forall v_{hb} \in V_{hb}^0, \tag{6}$$

in which $D_T(\cdot;\cdot,\cdot) : V_{hb}^0|_T \times V_{hb}^0|_T \times V_{hb}^0|_T \longrightarrow \mathbb{R}$ is the artificial diffusion operator given by

$$D_T(u_{hb}; u_{hb}, v_{hb}) = \int_T \xi_T\big(\kappa_h(u_{hb})\big) \boldsymbol{\nabla} u_{hb} \cdot \boldsymbol{\nabla} v_{hb} \, d\Omega, \tag{7}$$

where $\kappa_h : V_{hb}^0 \longrightarrow V_h^0$ is a linear projection operator, such that $\kappa_h(w_{hb}) = w_h$ with $(id - \kappa_h)(w_{hb}) = w_b \in V_b$ and id is the identity operator in V_{hb}^0 [6]. The artificial diffusion at each element $T \in \mathcal{T}_h$ is given by

$$\xi_T(u_h) = \begin{cases} \mu(h_T) \dfrac{\|R(u_h)\|_{0,T}}{\eta + \tau} \ , & \text{if } \ Pe_T > 1 \ , \\ \quad \text{with } \ \eta = \|u_h\|_{1,T}, \ \text{ if } \ \sigma > 0; \quad \text{or } \quad \eta = \|\boldsymbol{\nabla} u_h\|_{0,T}, \ \text{ if } \ \sigma = 0 \ , \\ 0, \quad \text{otherwise} \ , \end{cases} \tag{8}$$

where $\tau > 0$ is an appropriate constant. In (8), $Pe_T = \|\boldsymbol{\beta}\|_{0,T} h_T / 2\epsilon$ is the local Péclet number, $\mu(h_T) = \mathcal{O}(h_T) > 0$ is the local subgrid characteristic length scale satisfying $\mu(h_T) \leq \mu(h) = \max\{\mu(h_T);\ T \in \mathcal{T}_h\}$, and $R(u_h) = -\epsilon \Delta u_h + \boldsymbol{\beta} \cdot \boldsymbol{\nabla} u_h + \sigma u_h - f$ is the residual of the resolved scale solution. The latter expression simplifies when $u_h|_T \in \mathbb{P}_1(T)$, which is the case considered here. Thus, henceforth we will use $R(u_h) = \boldsymbol{\beta} \cdot \boldsymbol{\nabla} u_h + \sigma u_h - f$. Note that the new-DD operator (7) introduces a nonlinearity into the formulation (6) since it depends on the residual of the resolved scale solution. The artificial diffusion (8), that depends on the $T \in \mathcal{T}_h$, regulates the amount of stabilization, being larger where the resolved solution is less accurate and vanishing otherwise. We remark that, in the latter case, the Galerkin method enriched with bubble functions is automatically recovered. It is also worth mentioning that the new-DD method can handle reaction-diffusion problems by replacing the condition $Pe_T > 1$ with $\|\boldsymbol{\nabla} u_h\|_{0,T} > 10^{-5}$, as proposed in [20].

We solve (6) by using the iterative process developed in [20] to improve convergence. The actual artificial diffusion in each $T \in \mathcal{T}_h$ in the iteration $k+1$ is defined by combining values from two consecutive iterations in the form $\xi_T^{k+1} = \omega \hat{\xi}_T^{k+1} + (1-\omega) {\xi_T}^k$, with $\omega = 0.5$ and $\hat{\xi}^0 = 0.0$. The quantity $\hat{\xi}_T^{k+1}$ is set equal to $\xi_T^{k+1}(u_h^k)$, which is evaluated using Eq. (8), with $\mu(h_T) = h_T = \sqrt{meas_2(T)}$, in which $meas_2(T)$ is the area of the element T. The convergence of the iterative process is reached when $\left(\left\| (u_h^{k+1} - u_h^k)/u_h^{k+1} \right\|_\infty < 10^{-6} \right)$, limited to a maximum number of 30 nonlinear iterations. Moreover, we also integrate a strategy that sets the damping factor ω equal to zero when $\|R(u_h^k)\|_{0,T}$ is close enough to $\|R(u_h^{k-1})\|_{0,T}$, with a threshold of 20% for the relative error between these residuals.

3 Numerical Results

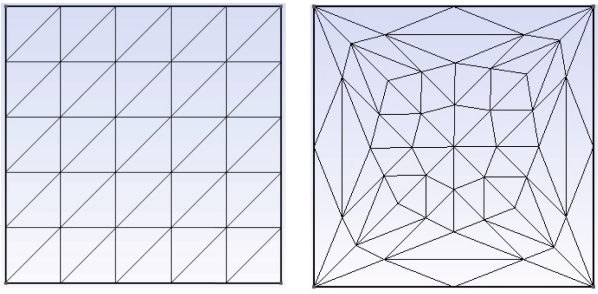
We investigate the numerical properties of the new-DD method for 2D transport problems with smooth solutions and in the presence of layers, using both structured and unstructured mesh, and different values for τ. We numerically evaluate the convergence rates measured using different norms, and then we analyze advection-dominated and reaction-dominated transport problems whose solutions have regions with strong gradients. We analyze the quality of the solutions for three values of the parameter τ: a small constant value $\tau = 10^{-5}$, related to the experiments showed in [20]; $\tau = 1$, as proposed in [15], and a locally problem-dependent value defined as $\tau = \tau_T = \max\{\|f\|_{0,T}, 10^{-5}\}$.

3.1 Convergence Rates

First, we investigate convergence rates in the $L^2(\Omega)$, $H^1(\Omega)$, and the energy norms for transport regimes ranging from advection to diffusion dominated problems with or without reaction term, for first-order interpolating polynomials ($\mathbb{P}_1$). Simulations were performed on one structured grid (Grid1) that were uniformly refined, and on one unstructured grid with obtuse triangles (Grid2) generated and refined using Gmsh [5]. Mesh patterns are illustrated in Fig. 1. We consider the following smooth solution

$$u(x, y) = 100x^2(1 - x)^2y(1 - y)(1 - 2y) \tag{9}$$

where the source term f is defined to satisfy Eq. (1), with $\boldsymbol{\beta} = (3, 2)^T$ and parameter combinations of $\sigma = 0$ or $\sigma = 1$, and $\epsilon = 10^{-6}$ or $\epsilon = 10$. Errors in $L^2(\Omega)$ ($\|\cdot\|_0$), $H^1(\Omega)$ ($\|\cdot\|_1$), and the energy ($\|\cdot\|_E$) norms (recalling that $\|v\|_E = \left(\epsilon|v|_1^2 + \sigma\|v\|_0^2\right)^{1/2}$) were evaluated for both grids and are reported in Table 1 using $\tau = 10^{-5}$, $\tau = \max\{\|f\|_{0,T}, 10^{-5}\}$ named as τ_T, and $\tau = 1$.



(a) Grid1 (b) Grid2

Fig. 1. Mesh patterns used in the numerical experiments.

Observe that optimal convergence rates in the $L^2(\Omega)$, $H^1(\Omega)$, and the energy norms are independently of the grid pattern, for all values of τ. Also, the order

of convergence in the energy norm is similar to that in the $L^2(\Omega)$ norm when $\epsilon = 10^{-6}$ and $\sigma = 1$. This means that the zero-order term outweighs the first-order term, which does not happen in the cases with $\sigma = 0$. It is also possible to notice a decrease in the convergence rates obtained with Grid2. However, the errors associated with the unstructured Grid2 are slightly the smallest errors for all cases. In particular, we plotted the errors against mesh size on a log–log scale in Fig. 2, for $\epsilon = 10^{-6}$, $\sigma = 0$, and τ_T. Overall, the influence of τ on the convergence orders across the grids is small, and optimal orders of convergence is sustained. However, for $\tau = \tau_T$ and $\tau = 1$, we may note a slight decrease of the convergence rate for solutions obtained with Grid2 and $\sigma = 1$ (see Table 1). Such mesh-dependence on the method is still a topic under investigation.

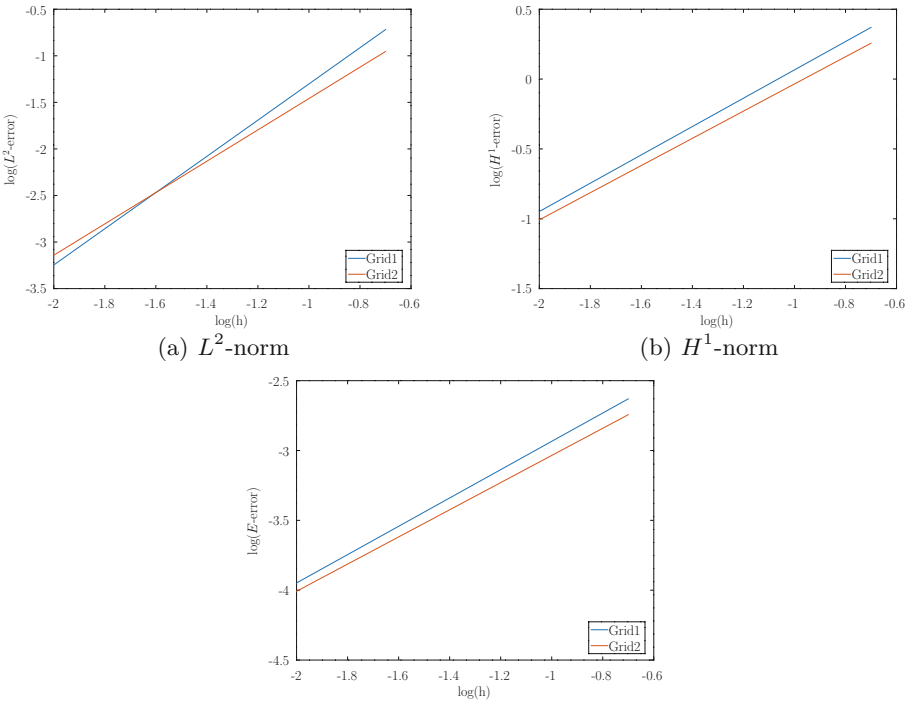
Table 1. Convergence rates for the numerical solution of (9).

τ	σ	Grid	$\epsilon = 10^{-6}$			$\epsilon = 10$		
			$\|u-u_h\|_0$	$\|u-u_h\|_1$	$\|u-u_h\|_E$	$\|u-u_h\|_0$	$\|u-u_h\|_1$	$\|u-u_h\|_E$
10^{-5}	0	Grid1	1.99	1.04	1.04	1.99	0.99	0.99
		Grid2	1.95	1.09	1.09	1.77	0.93	0.93
	1	Grid1	2.00	1.03	1.99	1.99	0.99	0.99
		Grid2	1.96	1.09	1.95	1.77	0.93	0.93
τ_T	0	Grid1	1.94	1.01	1.01	1.99	0.99	0.99
		Grid2	1.68	0.97	0.97	1.77	0.93	0.93
	1	Grid1	1.95	1.01	1.94	1.99	0.99	0.99
		Grid2	1.70	0.97	1.70	1.77	0.93	0.93
1	0	Grid1	2.03	1.00	0.90	1.99	0.99	0.99
		Grid2	1.44	0.95	0.95	1.77	0.93	0.93
	1	Grid1	2.03	1.00	2.01	1.99	0.99	0.99
		Grid2	1.43	0.95	1.43	1.77	0.93	0.93

3.2 Solution with Two Internal Layers

We now consider an advection dominated advection-diffusion problem, first presented in [11], with new-DD artificial diffusion calculated using (8). The model is defined in the unit square domain $\Omega = (0,1)^2$, where $\boldsymbol{\beta} = (1,0)^T$, $\sigma = 0$, $\epsilon = 10^{-8}$, and $f(x,y) = 16(1-2x)$ if $(x,y) \in [0.25, 0.75]^2$ and zero otherwise. Homogeneous Dirichlet boundary conditions are considered on Γ. The exact solution depicted in Fig. 3(a) is equal to zero everywhere but in $(0.25, 0.75)^2$, where it is close to the parabolic function $u = (4x-1)(3-4x)$ with interior layers at $(0.25, 0.75) \times \{0.25\}$ and $(0.25, 0.75) \times \{0.75\}$.

The quality of the new-DD solutions are evaluated based on measures of spurious oscillations given by both undershoots and overshoots, as the ones shown by the SUPG (Streamline Upwind Petrov-Galerkin) solution in Fig. 3(b), for



(a) L^2-norm (b) H^1-norm

(c) E-norm

Fig. 2. Convergence rates in the $L^2(\Omega)$, $H^1(\Omega)$, and the energy norms for the problem with $\epsilon = 10^{-6}$, $\sigma = 0$, and using τ_T.

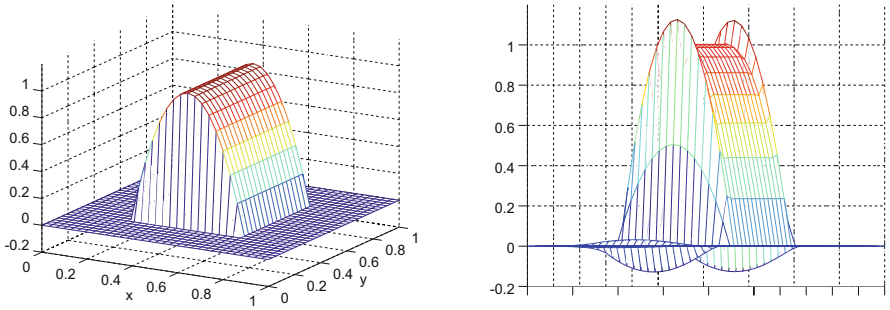
which the plane $z = 0$ was reduced to a line. Of note, the SUPG solution, implemented as in [2], was given for comparison. In Fig. 4, we compare the new-DD solutions for $\tau = 10^{-5}$ and $\tau = 1$, using a mesh with pattern Grid1 with 32×32 divisions in each direction. Both solutions are quite satisfactory, with the one obtained with $\tau = 1$ almost completely precluding spurious modes.

To observe the impact of τ in the solutions, we can accurately assess the amount of spurious oscillations in the discrete solution u_h by defining

$$min := - \min_{0.4 \le x \le 0.6} u_h(x, y), \quad diff := \max_{x \ge 0.8} u_h(x, y) - \min_{x \ge 0.8} u_h(x, y) \ , \qquad (10)$$

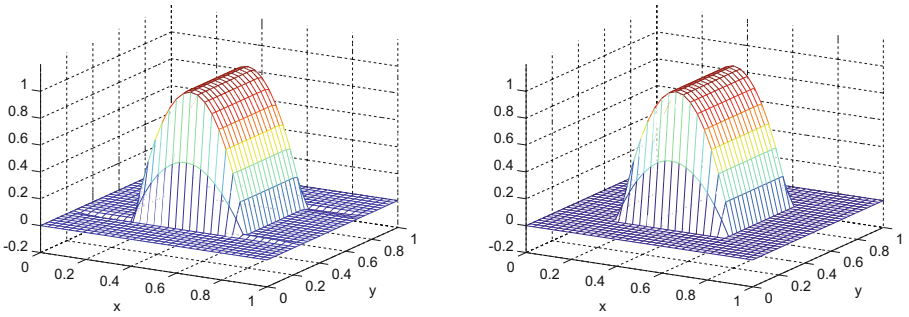
where $y \in [0, 1]$, and $\min u_h$ and $\max u_h$ are computed using values of u_h at the vertices of the mesh. Thus, as defined in [13], the *min* values measure the undershoots along the interior layers, while the *diff* values compare the magnitude of the discrete solutions in a region downstream from the layers, where it should vanish ($x \ge 0.8$). In Table 2, we show *min* and *diff* values for the new-DD method using different meshes (Grid1) with 16×16, 32×32 and 64×64 divisions, as well as different values for τ. Specifically, we set $\tau = 10^{-5}, 0.1, 1$ and $\tau = \tau_T = \max\{\|f\|_{0,T}, 10^{-5}\}$. The smallest *diff* value was attained with

$\tau = 1$, except for the more refined mesh; in all cases, the *min* values were less than 2×10^{-5}. Independently of the τ value, the new-DD method could handle this highly complex problem and yielded quite satisfactory solutions. Of note, the solution obtained with τ_T is quite similar to that using $\tau = 10^{-5}$.



(a) solution u (b) SUPG

Fig. 3. Two internal layers problem: solution u and SUPG solution using a mesh with pattern Grid1 with 32×32 cells.



(a) $\tau = 10^{-5}$ (b) $\tau = 1$

Fig. 4. Two internal layers problem: new-DD solutions using a mesh with 32×32 divisions and $\tau = 10^{-5}$ (a) and $\tau = 1$ (b).

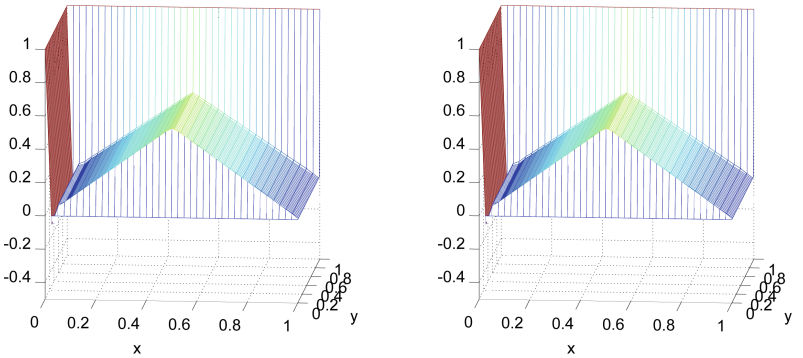
3.3 Reaction-Diffusion Problem

This is a reaction-diffusion problem, null velocity ($\boldsymbol{\beta} = (0, 0)$), characterized by dominance of reactive effects with two boundary layers. The problem is defined in the square region $\Omega = [0, 1] \times [0, 1]$, with $\epsilon = 10^{-6}$ and $\sigma = 1$, and source term given by

$$f(x, 0) = \begin{cases} x, & for \;\; x \leq -0.5; \\ 1 - x, & for \;\; x > 0.5. \end{cases}$$

Table 2. The *min* and *diff* values obtained using three different meshes and different values for τ.

	τ	16×16	32×32	64×64
min	10^{-5}	8.03×10^{-11}	1.08×10^{-12}	2.18×10^{-10}
	τ_T	7.82×10^{-11}	1.02×10^{-12}	2.18×10^{-10}
	0.1	5.23×10^{-11}	1.01×10^{-9}	1.62×10^{-8}
	1	1.03×10^{-6}	4.28×10^{-6}	1.45×10^{-5}
diff	10^{-5}	1.42×10^{-2}	6.81×10^{-2}	8.51×10^{-2}
	τ_T	1.56×10^{-2}	6.23×10^{-2}	8.39×10^{-2}
	0.1	9.24×10^{-3}	3.46×10^{-3}	1.02×10^{-3}
	1	9.05×10^{-4}	1.62×10^{-4}	1.28×10^{-4}



(a) $\tau = 10^{-5}$ (b) τ_T

(c) $\tau = 1$ (d) SUPG

Fig. 5. Reaction-diffusion flow field: new-DD and SUPG solutions.

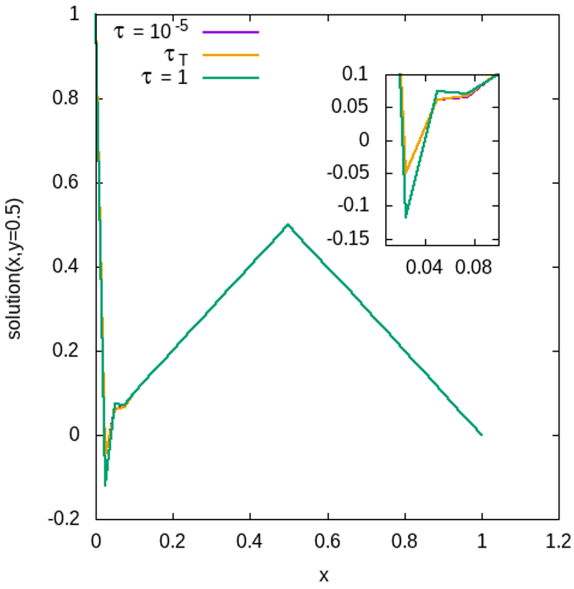
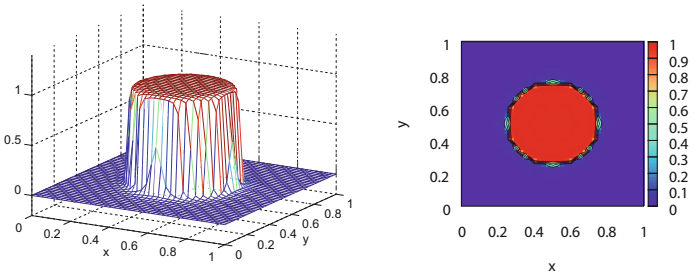


Fig. 6. Reaction-diffusion flow field: solution profiles for $0 \leq x \leq 1$ and $y = 0.5$.

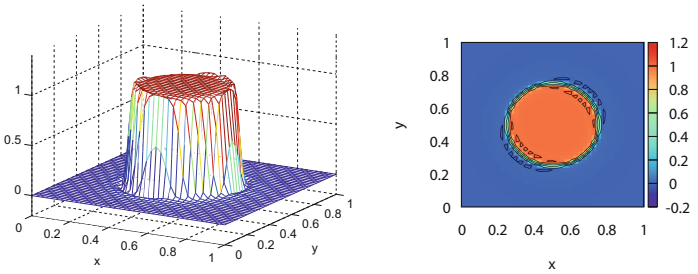
Dirichlet boundary conditions are assigned to the boundary: $u(0, y) = 1$ for $0 \leq y \leq 1$, $u(x, 1) = 1$ for $0 \leq x \leq 1$ and $u(x, 0) = 0$ for $0 < x \leq 1$. Figures 5(a), 5(b) and 5(c) show the three-dimensional structure plots of new-DD solutions for a mesh (Grid1) with 40×40 division using $\tau = 10^{-5}$, $\tau = \tau_T = \max\{\|f\|_{0,T}, 10^{-5}\}$ and $\tau = 1$, respectively. Here, also for comparison, we show in Fig. 5(d) the SUPG solution as calculated in [2]. All new-DD solutions show very small smearing and almost the suppression of both overshoots and undershoots. The numerical dissipation for all τ values can be better compared in the solution profiles for $0 \leq x \leq 1$ and $y = 0.5$, see Fig. 6. Clearly, the new-DD solution with $\tau = 1$ presents the biggest amount of overshoots at the left boundary, while the other new-DD solutions produce qualitatively better solutions. As in the last example, the new-DD solutions with $\tau = 10^{-5}$ and τ_T are practically the same and they yield qualitatively excellent solutions.

3.4 2D Advection-Diffusion-Reaction Problem

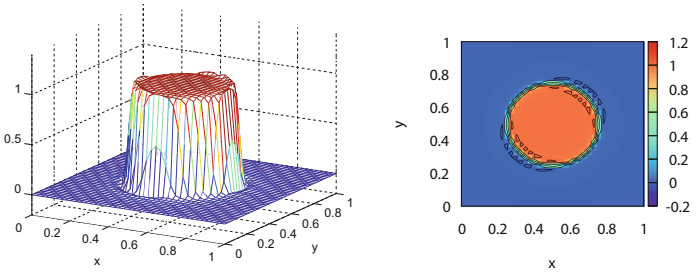
Now, we examine an advection dominated problem that models a "rotating pulse" [3,10], also with known exact solution but reaction term not null ($\sigma = 2$), i.e., the artificial diffusion being defined in (8). This problem is particularly interesting since the width of the internal transition layer is very thin ($\mathcal{O}(\epsilon^{1/2})$) and its alignment with the mesh elements is not constant. The exact solution,



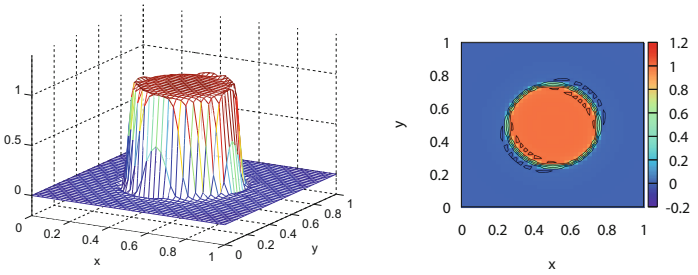
(a) Elevation and contour curve: exact solution.



(b) Elevation and contour curve: DD solution with $\tau = 10^{-5}$.



(c) Elevation and contour curve: DD solution with τ_T.



(d) Elevation and contour curve: DD solution with $\tau = 1$.

Fig. 7. Solutions of the "rotating pulse" problem for a mesh with 40×40 cells, $\tau = 10^{-5}$, τ_T and $\tau = 1$.

shown in Fig. 7(a), depicts a circular region where $u = 1$ is separated by a sharp transition from the rest of the domain, where $u = 0$. It is defined by

$$u = \frac{1}{2} + \frac{1}{\pi}\text{arctg}\left[1000(0.25^2 - (x-0.5)^2 - (y-0.5)^2)\right]. \tag{11}$$

The problem, in the unit square domain, uses $\epsilon = 10^{-4}$, $\sigma = 2$, and the components of the velocity field are

$$\begin{cases} \beta_x = -2(y-1)\left(0.25^2 - (x-0.5)^2 - (y-0.5)^2\right), \\ \beta_y = \quad 2(x-1)\left(0.25^2 - (x-0.5)^2 - (y-0.5)^2\right), \end{cases}$$

if $0 \leq (x-0.5)^2 - (y-0.5)^2 \leq 0.25^2$, and $\beta_x = \beta_y = 0$ otherwise. The source term f and Dirichlet boundary conditions are chosen appropriately to satisfy (11). The new-DD solutions with $\tau = 10^{-5}$, $\tau = \tau_T = \max\{\|f\|_{0,T}, 10^{-5}\}$ and $\tau = 1$ are presented in Figs. 7(b)–7(c). In this example, observe that all new-DD solutions are qualitatively similar. They can represent the region of high gradient with moderate smearing and some small localized oscillations probably related to the mesh pattern. Such issues can be better observed confronting the level curves. Note that the impact of τ on the solutions is undetectable in this problem.

4 Conclusions

This work focus on the stability and convergence properties of the new-DD method developed and analyzed in [18], a consistent method that effectively adds extra stability through a nonlinear operator acting in all scales of the discretization. This variant of the Dynamic Diffusion (DD) method [20] is defined via a new design for the nonnegative, upper bounded nonlinear artificial diffusion operator. In [18], it was theoretically proved that the new-DD method has a convergence rate of $\mathcal{O}(h^{1/2})$ in the energy norm. Moreover, defining $\tau = 10^{-5}$, optimal convergence rates in the $L^2(\Omega)$, $H^1(\Omega)$, and energy norms were numerically shown for advection- and diffusion-dominated problems with smooth solutions. Of note, this artificial diffusion relies on a problem dependent parameter that plays a key role on its upper boundedness. Thus, focusing on those numerical aspects, the objective here is a preliminary evaluation of how the new diffusion operator impact the solution of 2D transport problems with smooth solutions and in the presence of layers.

Our numerical experiments have shown that the new-DD method presents robust stabilization and convergence properties, and the accuracy of the method is not very sensitive to the choice of parameter τ. Specifically, here we considered small constant values of τ, $\tau = 10^{-5}, 0.1, 1$, and also a locally defined problem-dependent value, $\tau = \tau_T = \max\{\|f\|_{0,T}, 10^{-5}\}$. The convergence rates were obtained using both structured (Grid1) and unstructured (Grid2) meshes, for the problem with smooth solution. We solved an advection dominated problem with two internal layers, a reaction-diffusion problem characterized by dominance

of reactive effects with also two boundary layers, and an advection dominated problem that models a "rotating pulse", where the width of the internal transition layer is very thin and its alignment with the mesh elements is not constant. For all problems using the mesh pattern of Grid1, the new-DD solutions with $\tau = 10^{-5}$ and $\tau = \tau_T$ are practically the same and they yield qualitatively excellent solutions. In particular, we noted that the impact of τ on the new-DD solutions is undetectable in the "rotating pulse" problem. However, this is not the case for the others two problems with sharp layers, where the impact of τ is more significant. For instance, we have qualitatively better solutions using $\tau = 1$ in the two internal layers problem. However, the reaction-diffusion solution with $\tau = 1$ presents the biggest amount of overshoots at the left boundary. Overall, we consider that the new-DD method is robust for a wide scope of transport problems, showing potential for interesting future works. Possible extensions include the use of mesh adaptivity and high order approximations as well as extension for more involved problems, such as compressible and incompressible fluid flows.

Acknowledgments. This work was supported by the Foundation for Research Support of Espírito Santo (FAPES) under Grant 181/2017.

References

1. Arruda, N., Almeida, R., do Carmo, E.D.: Dynamic diffusion formulation for advection dominated transport problems. Mecánica Computacional **29**, 2011–2025 (2010)
2. Brooks, A., Hughes, T.: Streamline upwind/Petrov-Galerkin formulations for convection dominated flows with particular emphasis on the incompressible Navier-Stokes equations. Comput. Methods Appl. Mech. Eng. **32**, 199–259 (1982)
3. Cawood, M., Ervin, V., Layton, W., Maubach, J.: Adaptive defect correction methods for convection dominated, convection diffusion problems. J. Comput. Appl. Math. **116**(1), 1–21 (2000)
4. Galeão, A., do Carmo, E.D.: A consistent approximate upwind Petrov-Galerkin method for convection-dominated. Comput. Methods Appl. Mech. Eng. **10**, 83–95 (1988)
5. Geuzaine, C., Remacle, J.F.: GMSH: a 3-D finite element mesh generator with built-in pre- and post-processing facilities. Int. J. Numer. Meth. Eng. **79**(11), 1309–1331 (2009)
6. Guermond, J.L.: Stabilization of Galerkin approximations of transport equation by subgrid modeling. Math. Model. Num. Anal. **33**, 1293–1316 (1999)
7. Guermond, J.L.: Subgrid stabilization of Galerkin approximations of linear monotone operators. IMA J. Numer. Anal. **21**, 165–197 (2001)
8. Hughes, T.J.R., Scovazzi, G., Franca, L.P.: Multiscale and Stabilized Methods, pp. 1–64. American Cancer Society (2017). https://doi.org/10.1002/9781119176817.ecm2051
9. Hughes, T., Feijoo, G., Luca, M., Jean-Baptiste, Q.: The variational multiscale method - a paradigm for computational mechanics. Comput. Methods Appl. Mech. Eng. **166**, 3–24 (1998)
10. Iliescu, T.: Genuinely nonlinear models for convection-dominated problems. Comput. Math. Appl. **48**(10–11), 1677–1692 (2004)

11. John, V., Knobloch, P.: A computational comparison of methods diminishing spurious oscillations in finite element solutions of convection-diffusion equations. In: Proceedings of the International Conference Programs and Algorithms of Numerical Mathematics, vol. 13, pp. 122–136. Academy of Sciences of the Czech Republic (2006)
12. John, V., Knobloch, P.: On spurious oscillations at layers diminishing (SOLD) methods for convection-diffusion equations: part I - a review. Comput. Methods Appl. Mech. Eng. **196**(17–20), 2197–2215 (2007)
13. John, V., Knobloch, P.: On spurious oscillations at layers diminishing (SOLD) methods for convection-diffusion equations: part II - analysis for P1 and Q1 finite elements. Comput. Methods Appl. Mech. Eng. **197**(21–24), 1997–2014 (2008)
14. Johnson, C., Navert, U., Pitkäranta, J.: Finite element methods for linear hyperbolic problems. Comput. Methods Appl. Mech. Eng. **45**, 285–312 (1984)
15. Knopp, T., Lube, G., Rapin, G.: Stabilized finite element methods with shock capturing for advection-diffusion problems. Comput. Methods Appl. Mech. Eng. **191**(27), 2997–3013 (2002). https://doi.org/10.1016/S0045-7825(02)00222-0
16. Mallet, M.: A finite element method for computational fluid dynamics. Ph.D. thesis, Department of Civil Engineering, Stanford University (1985)
17. Santos, I.P., Almeida, R.C.: A nonlinear subgrid method for advection-diffusion problems. Comput. Methods Appl. Mech. Eng. **196**, 4771–4778 (2007)
18. Santos, I.P., Malta, S.M., Valli, A.M., Catabriga, L., Almeida, R.C.: Convergence analysis of a new dynamic diffusion method. Comput. Math. Appl. **98**, 1–9 (2021). https://doi.org/10.1016/j.camwa.2021.06.012
19. Valli, A., Catabriga, L., Santos, I., Coutinho, A., Almeida, R.: Multiscale dynamic diffusion method to solve advection-diffusion problems. In: XXXVI Ibero-Latin American Congress on Computational Methods in Engineering, Rio de Janeiro, RJ (2015)
20. Valli, A.M., Almeida, R.C., Santos, I.P., Catabriga, L., Malta, S.M., Coutinho, A.L.: A parameter-free dynamic diffusion method for advection-diffusion-reaction problems. Comput. Math. Appl. **75**(1), 307–321 (2018)